Experimental and numerical study on collapse of aged jacket platforms caused by corrosion or fatigue cracking

Chun Yan Ji, Hong Zhi Xue, Xing Hua Shi *, Oleg Gaidai

School of Naval Architecture and Ocean Engineering, Jiangsu University of Science and Technology, Zhenjiang, Jiangsu Province, PR China

ABSTRACT

This paper presents experimental and numerical study on the collapse of aged steel jackets, caused by corrosion or fatigue crack. The test models were manufactured in accordance with a scale ratio of a prototype jacket. Corrosion and crack damages calculated by some empirical equations were subjected to the model. The collapse experiments were performed for the intact, corroded and cracked jacket model. Damaged versus intact model comparison indicates that the crack and corrosion damage will degenerate the ultimate loads of structure significantly, and they will induce the different failure modes of the damaged jackets with intact one. The two damaged jackets are both failed by the crack tearing of the leg. Nonlinear finite element method was applied for experimental results validation. Numerical and experimental results are proven to be in a good agreement.

© 2016 Elsevier Ltd. All rights reserved.

1. Introduction

Steel jackets have been widely used in offshore oil industry in recent 20 years [1]. A number of over 15-years old jackets are still operational in Bohai bay of China, Mexican Gulf and Brazilian waters. As structures reach their design service lives, the fatigue life should be reassessed. The crack and corrosion play major role in structural aging, when jacket is subjected to environmental conditions like wave, wind and current loads. The ultimate strength will degrade with the crack and corrosion growth, causing risk of in the collapse and failure of the whole jacket, which will result in the loss of people, property and environment pollution. Some aspects of aged jacket fatigue life reassessment are presented in [2], in which the collapse assessment was performed by push-over method. One of the main motivations for this reassessment may be the safety or the need to extend their life.

The attention has been paid on the residual ultimate strength of the aged structure such as ship or elements for other marine structures and the intact jacket and other ones with crack and corrosion damages. Some works about global nonlinear collapse analyses of three-dimensional steel jacket were done using numerical method in [3]. The strength of tubular structure as ring-stiffened DT-joints in offshore jacket was predicted using finite element method [4]. Fatigue reliability analysis was done for the jacket support considering the corrosion and inspection [5]. The influence of crack and corrosion on the ultimate strength of aged ship was analyzed by Paik [6]. Reliability analysis of the ship subjected to the damages was also performed by Akpan [7] and Guedes Soares [8], but the resistance of the aged ship was simplified to the initial yielding that will underestimate or overestimate the ultimate strength. Besides, the collapse behavior of the ship plate under crack, corrosion and dent was assessed by the numerical and experimental methods [9], and also for the plate with pit corrosion using nonlinear finite element by Paik [10]. A general expression of the ultimate strength of the plate with any crack was derived based on the experimental and numerical results [11]. The experimental investigation for the scantling box girder under slight, average and severe corrosions was done recently [12,13].

The collapse behavior of the complex structure need to be studied by performing global nonlinear analyses of the overall structure [14,15]. The ultimate strength theory of ship structure has been developed during the last decades since Caldwell [16], including the progressive collapse method, idealized structural unit method and nonlinear finite element method [16–22]. And the experimental studies were carried out for the ultimate strength of the scantling ship hulls, as the box girder by Recking [23] and Nishihara [24], the model with residual stress and initial imperfections by Akhras [25], and the model under bend, shear and torsion by Ostapenko [26].

Nonlinear pushover approach is commonly used to determine the ultimate strength of framed structures [14,15,27]. Pushover analysis types can be categorized either static or dynamic [28]. In static analysis dynamic effects are either neglected or included as

a multiplier of the static forces, and the forces are applied as incremental static loads until the platform collapses.

In this paper static analysis is employed. Static pushover is a common methodology in jacket structural design. For the ultimate strength study of the steel jackets see e.g. [3]. The ultimate strength analysis is rather related to extreme loading; while crack and corrosion is another important cause of collapse, which needs to be studied in detail. Crack and corrosion prediction requires experimental as well as nonlinear numerical analysis.

To assess the collapse behavior of the aged jackets, three scantling models designed by the similar rules were tested respectively under quasi-static progressive loading including the intact, crack and corrosion model. In order to investigate the corrosion or crack effect on collapse of the jacket platform, two different experimental jacket models were compared, the intact one and the one damaged by corrosion and crack. The response in terms of load–displacement and load–strain relationship was given; showing the failure mode of the jacket platform, damaged by crack and corrosion. Numerical nonlinear finite element analysis of the damaged jacket was performed. Finally, numerical and experimental results were compared in this paper.

2. Fundamental theory

2.1. Crack model

To predict the crack propagation during the jacket lifetime, Paris–Erdogan equations are adopted [29]

$$\frac{da}{dN} = C(\Delta K)^m \tag{1}$$

$$\Delta K = Y \Delta \sigma \sqrt{\pi a} \tag{2}$$

where ΔK is the stress intensity factor, Y is the geometric factor, $\Delta \sigma$ is the stress range, a is the crack size, N is the number of loading cycles, C and m are material parameters, determined by the experiment.

For the small crack size Y can be assumed to be constant, then integration of Eqs. (1) and (2) leads to the following crack size estimate

$$a(T) = \begin{cases} \left[a_0^{1-m/2} + \left(1 - \frac{m}{2}\right) C (\Delta \sigma Y \sqrt{\pi})^m (T - T_0) \omega \right]^{\frac{1}{1-m/2}} & m \neq 2 \\ a_0 \exp C \Delta \sigma^2 Y^2 \pi (T - T_0) \omega & m = 2 \end{cases} \tag{3}$$

where a_0 is the initial crack size, $N = (T - T_0)\omega$ is the number of load cycles, T is the age of platform in years, T_0 is the time of initial crack generated.

2.2. Corrosion model

This paper assumes most common form of corrosion for mild and low alloy steels, namely uniform corrosion, where the loss of material is relatively uniform over the structural surface. Corrosion reduces the base shear capacity of platform by thinning the thickness of primary structural members; it reduces the ability of the structure to resist external loads. Different models of general corrosion growth have been suggested. Nonlinear model proposed in [30], enables accurate prediction of the thickness loss induced by corrosion. Basic equations of this model are

$$\begin{aligned} t_r(T) &= C_1 T_e^{C_2} \\ r_r(T) &= C_1 C_2 T_e^{C_2 - 1} \end{aligned} \tag{4}$$

where $t_r(T)$ is the corrosion depth for loss of thickness in mm; $r_r(t)$ is the corrosion rate in mm/year, T_e is the exposure time in years, after breakdown of coating, which is taken as $T_e = T - T_c - T_t$; T_c is the life of coating in years, and T_t is the duration of transition in years which may be pessimistically taken as 0, C_1 and C_2 are coefficients to be determined by the statistical analysis of corrosion measurement data.

2.3. Ultimate strength with the damages

2.3.1. Nonlinear finite element method (NFEM)

In the Finite Element Analysis (FEA), the set of equations describing the structural behavior is

$$[k(\delta)]\{\delta\} - \{F\} = 0 \tag{5}$$

where k is the stiffness matrix of the structure, δ is the nodal displacements vector and F is the external nodal force vector.

The ultimate strength of the offshore jacket structure is studied by the NFEM, in which the geometrical and material nonlinearities are considered. The nonlinear equations as in Eq. (5) are solved by the incremental iteration method, described as

$$\begin{cases} \{\Delta \delta\}_m^i = \left[K_m^i \right]^{-1} \left(\{R_m\} - \left\{ F_m^i \right\} \right) = \left[K_m^i \right]^{-1} \left(\Delta R_m - \psi_m^i \right) \\ \left\{ \delta_i^{j+1} \right\} = \left\{ \delta_i^j \right\} + \left\{ \Delta \delta_i^j \right\} \end{cases} \tag{6}$$

where $\{R_m\}$ is the load vector at the mth step, $\left\{ F_m^i \right\}$ is the nodal force at the ith iteration, $\{\Delta R_m\}$ is the load incremental, $\left\{ \psi_m^i \right\}$ is the unbalance force after ith iteration.

2.3.2. Ultimate strength of offshore jacket with damages

In this section Euler beam theory is used to describe beam elements.

(1) For crack damage. The stiffness matrix K of the crack element, of which the effective area is reduced, can be described as [31]

$$[K]_{es} = \frac{a_1 EI}{L^3} \begin{bmatrix} 12a_2 & 6La_2 & -12a_2 & 6La_2 \\ 6La_2 & 4L^2 a_3 & -6La_2 & 2L^2 a_4 \\ -12a_2 & -6La_2 & 12a_2 & -6La_2 \\ 6La_2 & 2L^2 a_4 & -6La_2 & 4L^2 a_3 \end{bmatrix} \tag{7}$$

where I is the sectional inertia, $a_1 a_i < 1, i = 2, 3, 4$, are the parameters of the crack size.

(2) For corrosion damage. The stiffness matrix K of the corroded hollow circular element can be written as

$$[K]_e = \frac{EI}{L^3} \begin{bmatrix} 12 & 6L & -12 & 6L \\ 6L & 4L^2 & -6L & 2L^2 \\ -12 & -6L & 12 & -6L \\ 6L & 2L^2 & -6L & 4L^2 \end{bmatrix} \tag{8}$$

where the section inertia $I = \frac{\pi}{64} \left((D_{ou} - d(T))^4 - D_{in}^4 \right)$ for corrosion jacket; D_{ou}, D_{in} are outer and inner diameters respectively; $d(T)$ is the corrosion thickness.

In this paper, the FEM software ANSYS is used to perform nonlinear analysis. The jacket platform crack is modeled as discontinuous region with thin opening, shown in Fig. 1, while the corrosion modeled as the thickness loss of the element.
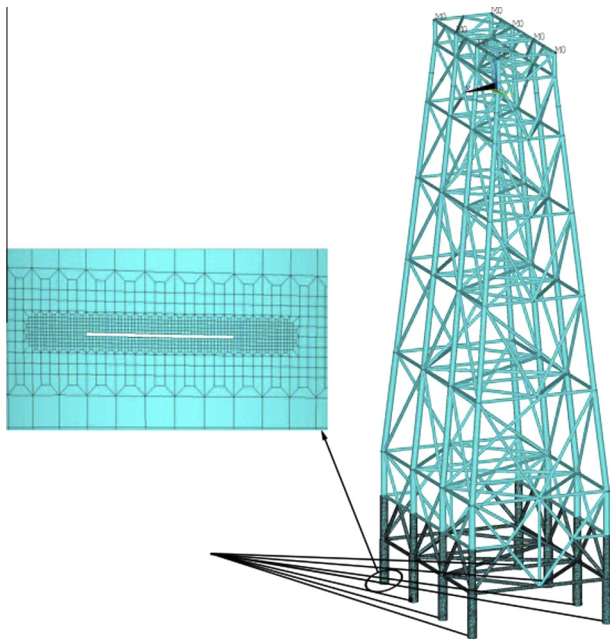
Fig. 1. The NFEM model of jacket and the crack model.

3. Experimental program

3.1. The jacket test model

An existing jacket platform installed in Gulf of Mexico is selected as the prototype, as shown in Fig. 3. The original jacket structure with the average working water depth of 105 m was constructed by 8 legs distributed rectangularly, fixing the whole structure to the seabed. The overall jacket height is 119 m. The principal dimensions and other parameters are listed in Table 1.

3.2. Crack and corrosion damage of the model in serving life

Fatigue crack and corrosion can change the global stiffness matrix K by thinning the structural thickness and reducing effective area of structural elements, which will induce the reduction of the ultimate strength of the jackets. The parameters of crack and corrosion models are given by [7,32], where $a_0 = 1.0$ mm, $m = 2.5$, $C = 1.16E-10$, $Y = 1.0$. There is no observation of the prototype jacket crack size. In this paper, the crack size is obtained by Eq. (3). For the lack of observation data, the current study adopted the maximum corrosion rate as 0.15 mm/year for submerged steel members and for members in the atmospheric zone as 0.05 mm/year [33], and the corrosion protection system is included. The data of the crack and corrosion varying with the serving life from 10 to 50 years are shown in Table 2.

3.3. Description of the tested models

3.3.1. The intact model

Three jacket models were tested: the intact model without corrosion and crack, the corrosion model in which corrosion occurs

Table 1
The principal dimensions and other parameters.

Total weight (t)	4665.3
Diameter of the catheters (m)	Ranged from 1.6 to 3
Thickness of the catheters (mm)	Ranged from 40 to 80
Damping ratio	0.04
Natural frequency (Hz)	0.564

Table 2
Damage data of structure varying with the serving life.

Serving life/years	Crack length/mm	Corrosion thickness/mm	
		Atmospheric	Submerged
10	4.77	0.02	0.18
15	9.51	0.15	0.97
20	18.97	0.45	2.25
25	37.84	0.97	3.71
30	75.47	1.73	5.21
35	150.51	2.69	6.71
40	300.15	3.83	8.21
45	598.56	5.10	9.71
50	1193.66	6.47	11.21

Table 3
The main scantlings of the tested models.

Elements	Leg	Pipe 1	Pipe 2	Pipe 3	Pipe 4	Braces
Diameter (mm)	75	60	50	50	40	25
Thickness (mm)	1.2	1.1	1.1	1.0	1.0	0.9

and the crack model where one crack occurs in the bottom of the each legs.

The similar guidelines of the model and the original structure on the basic mechanics characteristics are considered in the experimental model design. The similarities of geometry and stiffness that affect the ultimate strength are mainly satisfied with the scaling ratio of 1:40. The main scantlings of the tested model are showed in Table 3. The material parameters and stiffness of the tested model compared with original structures are shown in Table 4. It is found that the tested model is absolutely a scale model with the similarity of geometry and stiffness. The experimental model schematic diagram and the geometry dimensions are shown in Fig. 2. And the intact tested model is shown in Fig. 3b.

3.3.2. Crack model

Fig. 4 shows the tested crack model which is designed by applying initial cracks on the intact jacket model. In this tested model, the horizontal cracks are assumed to be produced in the joints of legs and horizontal braces induced by the fatigue under cycling loading condition of compress and tension. The ultimate strength of cracked jacket is investigated in this model. For this model, considering jackets serving 50 years, the crack length using Table 2 is estimated as 30 mm based on the geometric similarities ratios.

3.3.3. Corrosion model

The corrosion model shown in Fig. 5, has reduced thickness compared with the intact model. The corrosion in this tested model is induced via an electrochemical approach in which the corroded thickness can be achieved through the electrochemical time accurately in the laboratory. The corrosion model parameters and the damage value are shown in Table 5. Scantling and material are the same as for the intact tested model. The corrosion loss is 0.28 mm for submerged elements and 0.16 mm for atmospheric ones for the jackets serving 50 years, as shown in Table 2.

3.4. Experimental setup

Offshore jackets are built using pipes to fix main structure to seabed. According to API, the boundary conditions for the model are modeled as fixed constraints. The pre-loading process is made to eliminate the gaps between the tested model and the hydraulic machine. Before the formal test, the rearrange of the test setup has been done until every part in full contact.

Table 4
The material parameters and stiffness of the tested model compared with the original structure.

	Material	Elastic modulus	Poisson's ratio	Density	Stiffness
Original jacket	Steel	210 GPa	0.3	7800 kg/m^3	13546239.7
The tested model	Steel	210 GPa	0.3	7800 kg/m^3	339869.2
The scaling ratio	–	1:1	1:1	1:1	39.857:1
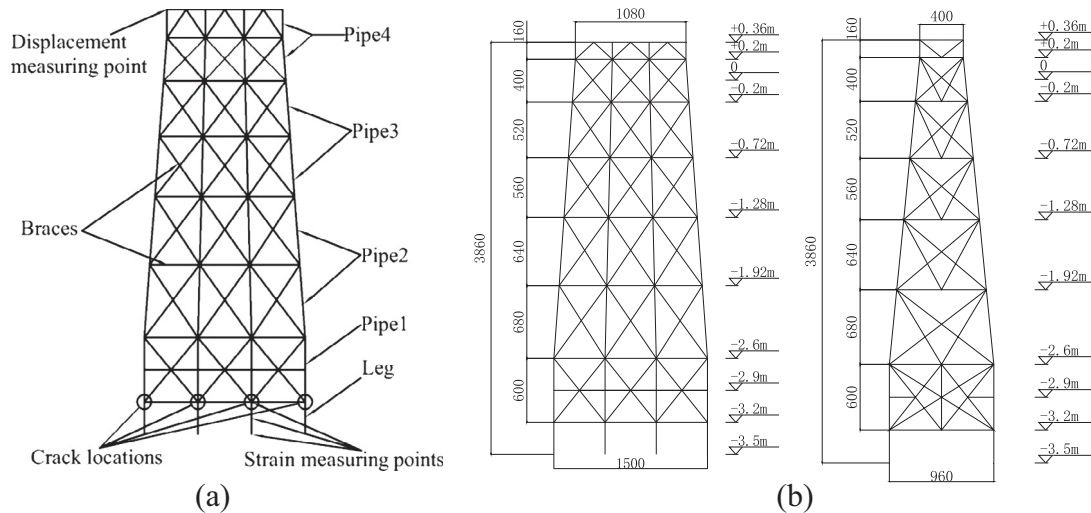
Fig. 2. The block of tested model and geometry dimensions. (a) Elements and crack location; (b) geometry dimensions.

For jacket offshore structure, the wave force presents main external environmental load; it is taken as a concentrated horizontal load at the water level in this test. The horizontal loads applied on the model increasingly, until the test model fails. The strains of each measuring point as shown in Fig. 7 were recorded. The displacement measuring points are shown in Fig. 2, and load measuring points were placed as shown in Fig. 6.

3.5. Loading sequence

When the test starts and the edge starts being displaced, large displacements occur under a small level of load. The pre-loading process should be made to eliminate the gaps of tested model, support and hydraulic machine, and rearrange the test setup until every part is in full contact. This load can be 15% of the maximum load that can be estimated by the numerical of theoretical methods. The model was applied loading in large incremental until 50% of the maximum load achieved in which only elastic deformation occurs. The strains, displacements and loading of each measuring point were recorded as the results. The offset is usually specified as a strain of 0.2%.

4. Experiment results

4.1. The ultimate strength of the intact model

The experimental load–displacement curve of the tested model is presented in Fig. 8, showing linear displacement increase, as the load increased progressively up to 35 kN. When the load approaches 40 kN, the increase of displacement becomes prominent, the increase of axial load becomes slower in this stage, and the permanent deformation appears. The load–displacement curve becomes nonlinear, and the material of the tested model is in plastic range after exceeding the ultimate strength (45.7 kN at the point A shown in Fig. 8). The unloading also begins after the point A; finally the jacket fails at the point B in Fig. 8. The deformations at the leg bottom are shown in Fig. 9. Fig. 9(a) gives the deformations at the collapse state, in which a small pit emerges in the leg pipe, and Fig. 9(b) gives the deformations at the failure state, where the large pit occurs.

4.2. The ultimate strength with crack

The failure process of the crack test model under progressive loading is shown in Fig. 10 by the load–displacement curve. It shows that the plastic deformation appears after the loading increases progressively to 26 kN, and the ultimate load is 31.5 kN. The unloading also begins after the point A. The resistance has degraded non-linearly from the point A to the point B in Fig. 10 and the crack observed propagated slowly in this stage. Resistance decreases rapidly from the point B to the point C, and the cracks in the legs are observed to spread rapidly. The whole model happens to collapse, when reaching the point C and proceeding to the point D. The tearing of crack was observed in the leg under tension results for the large damage and deformations in the stage between the points C and D. Starting from the point D, and proceeding to the point E, the resistance decreases rapidly again, leading to the whole structure failure at the point E. The deformation and damage of the crack model at the failure stage are shown in Fig. 11. Fig. 11 shows that the tearing has caused failure of the crack model, while the initial crack spread to almost half of the leg circumference.
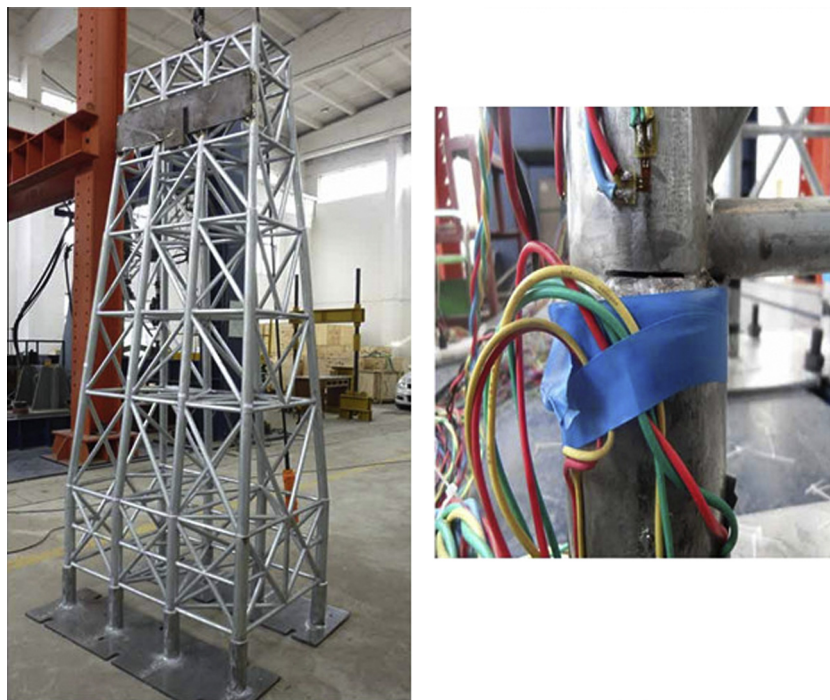
4.3. The ultimate strength with corrosion

As shown in Fig. 12, the load–displacement curve illustrates the progressive failure process of the corroded model. With increase of the external load, the corroded model achieves the maximum
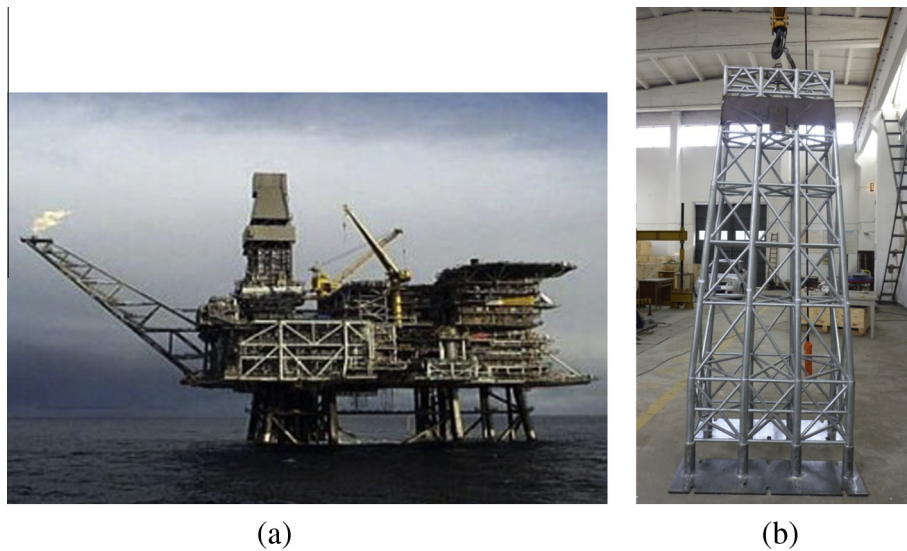
Fig. 3. The model of jacket. (a) Prototype; (b) test intact model.

Fig. 4. The cracked model of jacket.

resistance of 33.4 kN. After that, the unloading begins. From the point A to the point B in Fig. 12, the resistance of the model degrades significantly, while the appearance and propagation of the cracks is observed in the legs under tension in this stage. From the point B to the point C, the resistance decreases slowly, while the horizontal displacement of the test model increases rapidly. Cracks were observed to propagate rapidly as well, resulting in large deformation of the leg damaged circumference under compression, as shown in Fig. 13. The whole structure failed as the resistance degraded seriously, between points C and D. The failure mode is the tearing failure of the leg. The larger reduction of the pipe thickness is changing the failure mode of the platform, meaning that failure mode of platform can vary from being either the local structure tearing mode, or the global yield mode. The main

reason is that the stress increases and rearranges in the whole structure due to the thickness lose, especially in the joints of the legs and the braces, and with the increasing of the load, the high stress areas appear near the cracks. Rapid crack propagation caused the corroded model failure due to local tearing.

4.4. Comparison between the experimental results and numerical results

Series of FEM analyses were performed to simulate the ultimate state of intact and damaged jacket with cracks or corrosion. Results are shown in Figs. 14–16. Comparison between test and numerical load–displacement curves for three jackets models studied in this paper is shown in Fig. 17. Comparison results show that the
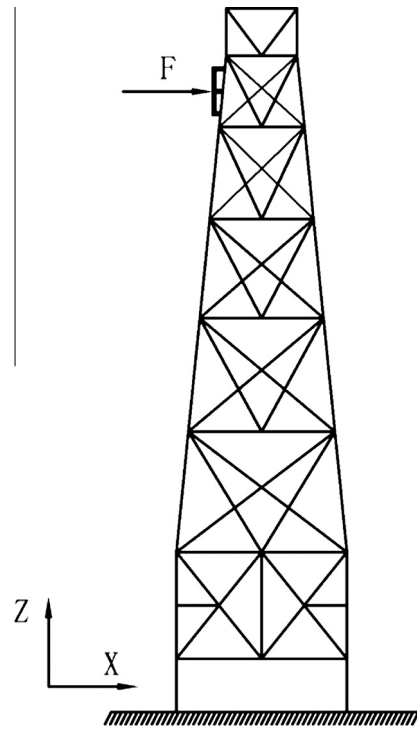
Fig. 5. The corrosion model of jacket.

Fig. 6. The loading and boundary of the test models.

stiffness of the platform model, obtained by numerical calculation is larger than the stiffness obtained by the test, before the model reaches its maximum resistance. This is mainly caused by ignoring the initial imperfections of the jacket models in the FE model by the numerical method, such as imprecise of machining (initial deformation and residual stress induced by manufacturing) and some uncertainty of material properties. Numerical FEM method presented in this paper can give good estimation results which are agreed with experiments for the ultimate strength of a steel jacket platform with corrosion or fatigue crack. The ultimate strength numerical and experimental results for the intact, crack and corroded jacket models are listed in Table 6. The relative deviations between numerical and experimental results are about 2.71%, 7.25% for intact and corroded model, and about 8% for the crack model.

Numerical FE method was not used to simulate the unloading process after the model reached its maximum resistance. Damage due to crack or corrosion may have significant influence on the structure collapse behavior. It was problematic to simulate effects of crack propagation or local structural deformation during the unloading process, using nonlinear FEM. Therefore significant differences during unloading path occurred between tests and FEM.

4.5. Experimental results discussion for three models

Fig. 18 shows a comparison of the load and displacement relationships between the intact, corrosion and crack model. Comparison shows that stiffness of the crack model and the cor-
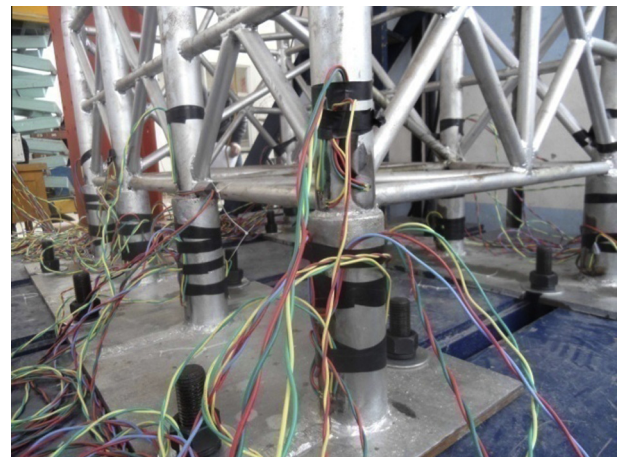

Fig. 7. The measuring points locations.

roded model is slightly less than that of the intact model before reaching the maximum bearing capacity. The ultimate strength of the crack model and the corroded model is significantly less than that of the intact model. The degradation of the crack model is more than 30% compared with the intact one, about 27% for the corrosion model. The latter indicates the corrosion and crack will significantly decrease the ultimate bearing capacity for an aged

Table 5
The geometric of the corrosion model.

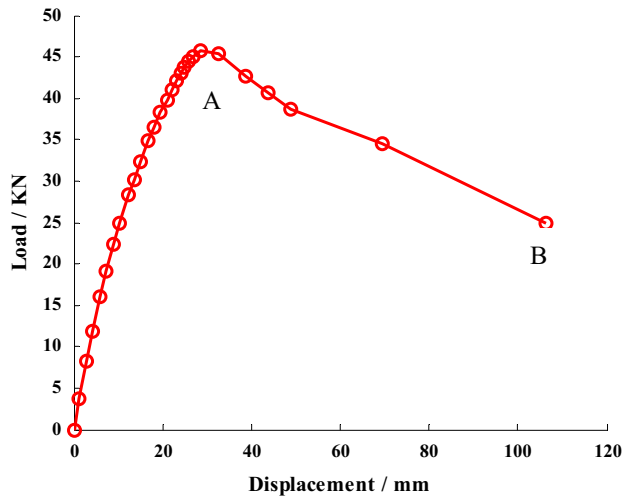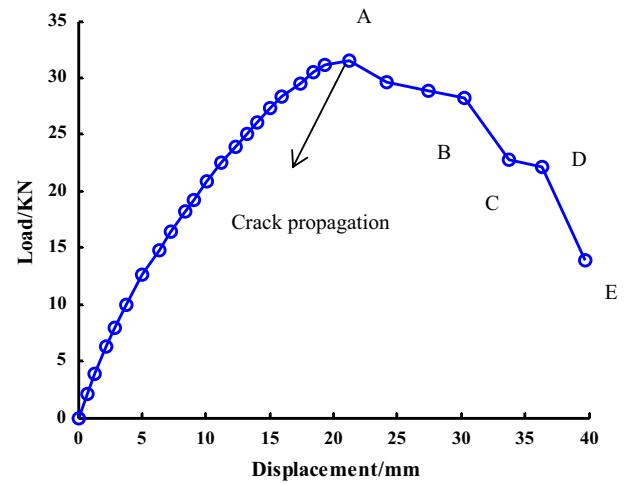| Elements	Leg	Pipe 1	Pipe 2	Pipe 3	Pipe 4	Horizontal braces and bracings
Diameter (mm)	75	60	50	50	40	25
Thickness (mm)	0.92	0.82	0.82	0.72	0.72 (for the submerged elements)	0.62 (for the submerged elements)
					0.94 (for the atmospheric elements)	0.74 (for the atmospheric elements)

Fig. 8. Load–displacement curve of the intact model.

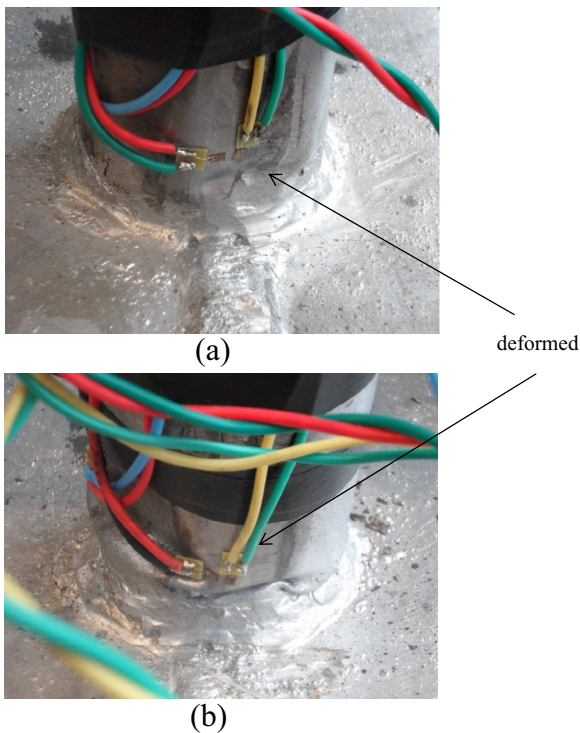Fig. 10. Load–displacement curve of the crack model.

Fig. 9. The deformed shape of legs of the intact model (a) at collapse; (b) at failure.

Fig. 11. Tearing deformation of the crack model at failure.
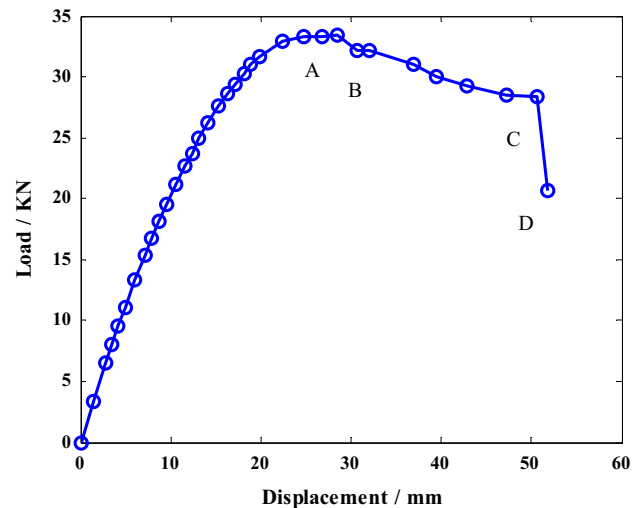
Fig. 12. Load–displacement curve of the corroded model.

platform. During the post-collapse process, stronger nonlinear mechanics have been observed for the crack model and the corroded model compared with the intact model.

5. Conclusions

Collapse behavior of an aged offshore jacket has been studied by experimental and numerical methods. Nonlinear finite element method was used to calculate the ultimate strength of an aged offshore jacket, taking into account effects of corrosion and crack. Effect of corrosion and crack on the ultimate strength of the jacket was studied for three jacket models, namely the intact model, the crack model and the corroded model. Models were designed to simulate an aged jacket with 50 years-service life according to the similar scaling rules of geometry and stiffness. Furthermore,
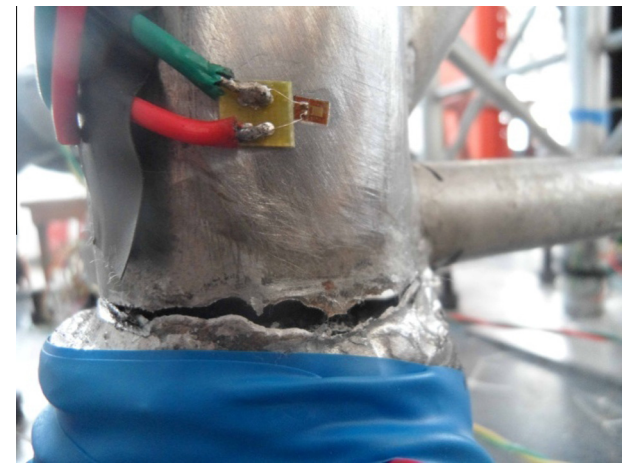
a series of tests were conducted, in order to validate numerical results. Based on test and numerical results, the following conclusions can be drawn:

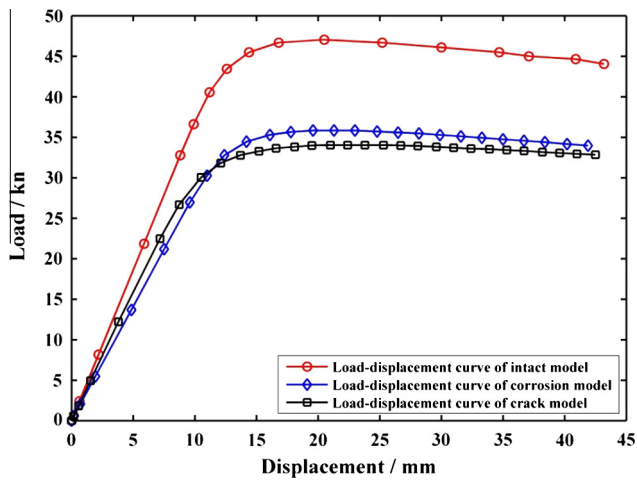**Fig. 13.** Crack tearing deformation of the corrosion model.

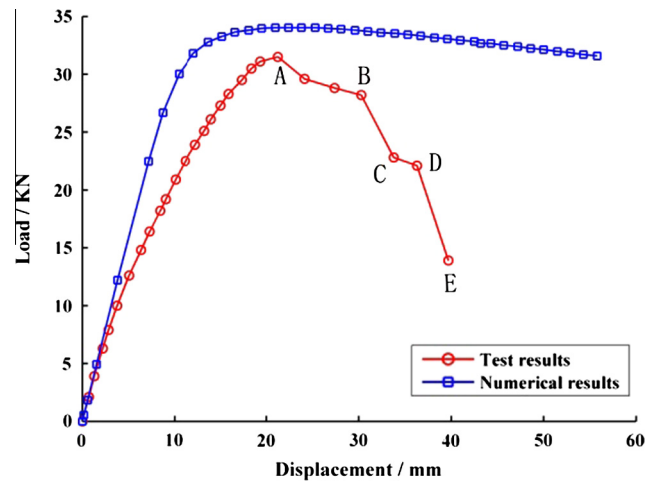**Fig. 14.** Numerical results.

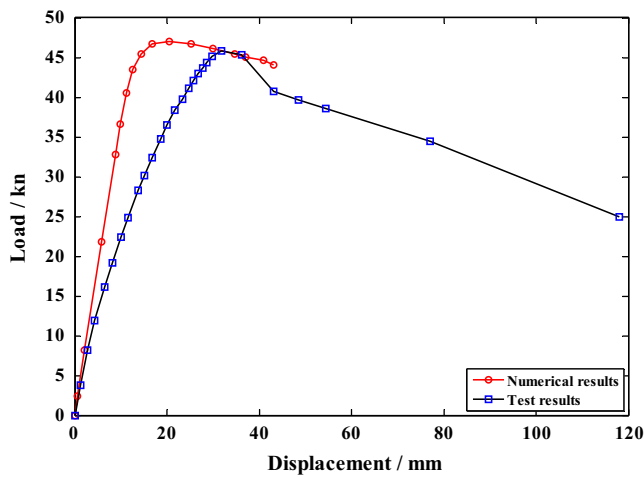**Fig. 16.** Comparison between the test and the numerical results of the crack model.

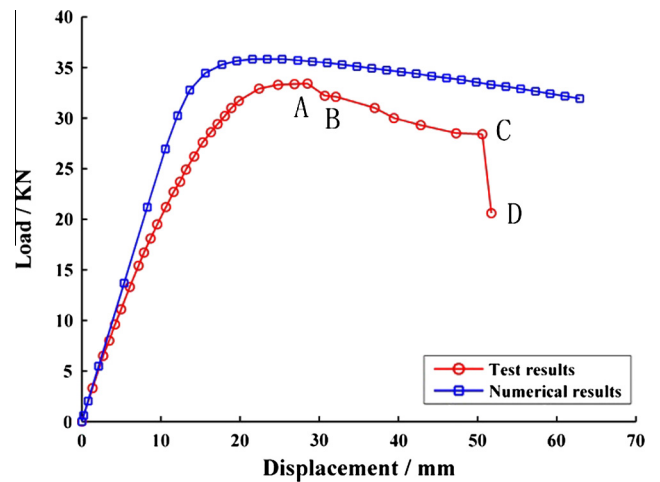**Fig. 15.** Comparison between the test and the numerical results of the intact model.

Fig. 17. Comparison between the test and the numerical results of the corroded model.

(1) Experimental aged jacket model was set up. Corrosion and crack significantly decreased the ultimate aged jacket capacity. Considering cracks without corrosion for an aged jacket with 50-years service life, the ultimate strength of the jacket was decreased more than 30%. Corrosion without crack model for an aged jacket with 50 years-service life, yielded about 27% decrease of the jacket ultimate strength. Since corrosion and crack act simultaneously on the real jacket in the sea, the ultimate strength of the jacket will decrease much more than that of crack and corrosion modeled separately.

Table 6
Results by numerical calculation and the tests of the ultimate strength of the jackets.

Model	Test (KN)	NFEM (KN)	Deviation (%)
Intact	45.8	47.04	2.71
Corrosion	33.4	35.82	7.25
Crack	31.5	34.02	8

(2) Experimental results show that the larger cracks or corrosion thickness change the failure mode of the jacket. Failure mode changes from a global yield for the intact jacket to a
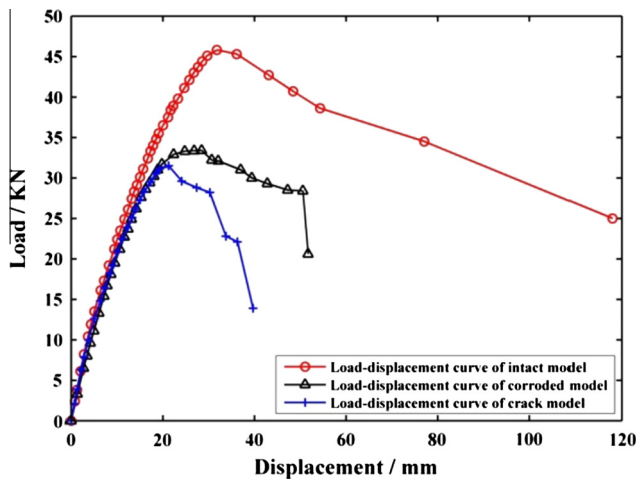
Fig. 18. Comparison between intact, corroded and crack models.

local tearing failure mode for the jacket with larger cracks or corrosion. The main reason is that the stress increases and rearranges in the whole structure due to the thickness lose for a corroded jacket, especially in the joints of the legs and the braces. With increase of the jacket load, high stress areas appear around cracks. Therefore jackets with either cracks or corrosion, will fail due to local tearing with rapid crack propagation.

(3) Deviations between the numerical and experimental results of the ultimate strength of are less than 10%. It was problematic for numerical FEM method to simulate accurately strongly nonlinear unloading process, after the model reached the maximum resistance.

Acknowledgements

References

[1] Wisch DJ. Fixed steel offshore structure design-past, present & future. In: Proceedings of the offshore technology conference. Houston, Texas; 1998. p. 317–23.
[2] Waegter J, Vissing-Jorgensen C, Thesbjerg L, Krenk S. Pushover analysis of framed offshore structures. In: Procs of the 17th international conference on offshore mechanics and arctic engineering; 1998. p. 1–6.
[3] Rodrigues PFN, Jacob BP. Collapse analysis of steel jacket structures for offshore oil exploitation. J Constr Steel Res 2005;61:1147–71.
[4] Lee MMK, Llewelyn-Parry A. Strength prediction for ring-stiffened DT-joints in offshore jacket structures. Eng Struct 2005;27:421–30.
[5] Dong W, Moan T, Gao Z. Fatigue reliability analysis of the jacket support structure for offshore wind turbine considering the effect of corrosion and inspection. Reliab Eng Syst Saf 2012;106:11–27.
[6] Paik JK, Thayamballi AK. Ultimate strength of ageing ships. Proc Inst Mech Eng, Part M: J Eng Marit Environ 2002:57–77.
[7] Akpan UO, Koko TS, Ayyub B, Dunbar TE. Risk assessment of ageing ship hull structures in the presence of corrosion and fatigue. Mar Struct 2002;15:211–31.
[8] Guedes Soares C, Garbatov Y. Reliability of maintained ship hull girders subjected to corrosion and fatigue. Struct Saf 1998;20:201–19.
[9] Paik J, Wang G, Thayamballi K, Lee J, Park Y. Time-dependent risk assessment of aging ships accounting for general/pit corrosion, fatigue cracking and local denting damage. ABS technical paters; 2003.
[10] Paik JK, Lee JM, Ko MJ. Ultimate shear strength of plate elements with pit corrosion wastage. Thin-Wall Struct 2004;42:1161–76.
[11] Paik J, Satish Kumar Y. Ultimate strength of cracked plate elements under axial compression or tension. Thin-Wall Struct 2005;43:237–72.
[12] Saad-Eldeen S, Garbatov Y, Guedes Soares C. Experimental assessment of the ultimate strength of a box girder subjected to severe corrosion. Mar Struct 2011;24:338–57.
[13] Saad-Eldeen S, Garbatov Y, Guedes Soares C. Ultimate strength assessment of corroded box girders. Ocean Eng 2013;58:34–47.
[14] Hellan O, Moan T, Drange S. Use of nonlinear pushover analyses in ultimate limit state design and integrity assessment of jacket structures. In: Procs of the int conf on the behaviour of offshore structures; 1994. p. 323–45.
[15] Kim S, Lee J, Park J. 3-D second-order plastic-hinge analysis accounting for local buckling. Eng Struct 2003;25:81–90.
[16] Caldwell J. Ultimate longitudinal strength. Trans RINA 1965;107:411–30.
[17] Nishihara S. Analysis of ultimate strength of stiffened rectangular plate (4th report)-on the ultimate bending moment of ship hull girder. J of Soc Naval Arch Jpn 1983;154:167–375.
[18] Smith C. Influence of local compressive failure on ultimate longitudinal strength of a ship's hull. In: Proceedings of the international symposium on practical designin shipbuilding (PRADS); 1977. p. 73–9.
[19] Ozguc O, Das P, Barltrop N. Analysis on the hull girder ultimate strength of a bulk carrier using simplified method based on an incremental-interactive approach. In: Proceedings of the 25th international conference on offshore mechanics and arctic engineering (OMAE 2006). San diego, OMAE2006-92338; 2006.
[20] Gordo J, Guedes Soares C. Approximate methods to evaluate the hull girder collapse strength. Mar Struct 1996;9:449–70.
[21] Paik JK, Kim BJ, Seo JK. Methods for ultimate limit state assessment of ships and ship-shaped offshore structures: part III hull girders. Ocean Eng 2008;35:281–6.
[22] Shi X, Teixeira AP, Zhang J, Guedes Soares C. Structural reliability analysis based on probabilistic response modelling using the maximum entropy method. Eng Struct 2014;70:106–16.
[23] Reckling K. Behaviour of box girder under bending and shear. ISSC committee II. 2. In: Proceedings of the 7th international ship and offshore structures congress (ISSC). Paris; 1979. p. 46–9.
[24] Nishihara S. Ultimate longitudinal strength of midship cross section. Naval Arch Ocean Eng 1984;22:200–14.
[25] Akhras G, Tremblay J. Finite strip analysis of a box girder simulating the hull of a ship. Struct Eng Mech 2003;15:225–38.
[26] Ostapenko A. Strength of ship hull girders under moment, shear and torque. In: Proceedings of symposium on extreme loads response. Arlington, Virginia, USA; 1981. p. 149–66.
[27] Stewart G, Efthymiou M, Vugts J. Ultimate strength and integrity assessment of fixed offshore platforms. In: Procs of the int conf on the behaviour of offshore structures; 1988.
[28] Wei K, Arwade SR, Myers AT. Incremental wind-wave analysis of the structural capacity of offshore wind turbine support structures under extreme loading. Eng Struct 2014;79:58–69.
[29] Guedes Soares C, Garbatov Y. Reliability of maintained ship hulls subjected to corrosion and fatigue under combined loading. J Construct Steel Res 1999;52:93–115.
[30] Qin S, Cui W. Effect of corrosion models on the time-dependent reliability of steel plated elements. Mar Struct 2003;16:15–34.
[31] Filho ELVC, Melo GPD, Fernandes V. Non linear dynamic crack model applied to state observers methodology for fanlt detection, localization and evaluation in a Cantilever beam. J Math Syst Sci 2012;2:384–92.
[32] Paik JK, Kim S Kyu, Lee S Kon. Probabilistic corrosion rate estimation model for longitudinal strength members of bulk carriers. Ocean Eng 1998;25:837–60.
[33] Melchers RE. Corrosion uncertainty modelling for steel structures. J Construct Steel Res 1999;52:3–19.